South East Asian J. of Mathematics and Mathematical Sciences
Vol. 16, No. 3 (2020), pp. 269-282

ISSN (Online): 2582-0850

ISSN (Print): 0972-7752

HOMOTOPY PERTURBATION METHOD FOR MHD BOUNDARY LAYER FLOW OVER A MOVING VERTICAL PLATE IN PRESENCE OF HEAT AND MASS TRANSFER

Manoj Kr. Sarma, Sujan Sinha and Bandita Das*

Department of Mathematics,
Assam downtown University, Guwahati - 781026, INDIA

E-mail : mksghy3009@gmail.com, mathssujangu@gmail.com

*Department of Mathematics,
Guwahati College, Bamunimaidam, Guwahati - 781021, INDIA

E-mail : banditadas1234@gmail.com

(**Received:** *Mar. 30, 2020* **Accepted:** *Sep. 16, 2020* **Published:** *Dec. 30, 2020)*

Abstract: The steady MHD boundary layer flow over a moving vertical plate with magnetic field and convective surface in presence of heat and mass transfer has been premeditated. Using He's Homotopy Perturbation Method (HPM), the system of non-linear ordinary differential equations governing the MHD boundary layer equations is solved. The influence of various significant physical parameters on the boundary layer flow is illustrated graphically with the physical interpretation. The obtained results point to the efficiency and convenience of the HPM. Utility of this model has been perceived in diverse industrial and chemical processes.

Keywords and Phrases: MHD, Heat Transfer, Mass Transfer, HPM, Schimdt number, Prandtl number.

2010 Mathematics Subject Classification: 76W05.

1. Introduction

Investigation of MHD boundary layer flow with heat and mass transfer has momentous applications in the fields of aeronautical plasma flows, nuclear reactor, magnetosphere, chemical engineering and electronics. Most of chemical engineering

progression like polymer extrusion processes and metallurgical involves cooling of a molten liquid. To improve the quality of the eventual creation, *Aziz*[1], *Chamkha* [2], *Cortell* [3], *Magyari* [6], *Makinde* [7], *Postelnicu* [8], *Tesfaye et. al* ([10], [11]), *White* [12], *Jhankal* [5], *He* [4], *Sinha et. al* [9] etc. have astounding contribution in solving various flow problems of assorted geometries. In [7], this problem was considered by a competent numerical technique. In order to prove those results of [7], the HPM is incorporated. In the meantime, the non-linear terms are expanded to Taylor's series of the Homotopy Parameter p.

2. Mathematical Formulation

The present study contemplates an MHD boundary layer flow over a moving vertical plate with heat and mass transfer of viscous in presence of magnetic field. The flow is supposed to be in x-axis which is along the direction of plate and y-axis is taken normal to it. Let u and v be the x and y components of fluid velocity respectively. The flow formation which describes the physical insight of the problem is given by Figure 1:

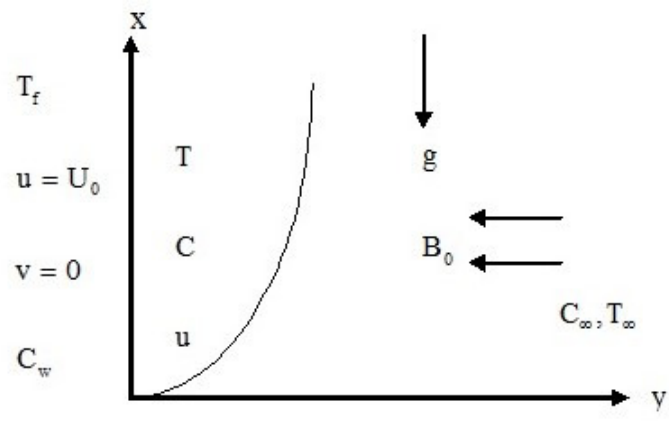

Figure 1

Using boundary layer and *Boussinesq's approximations*, the governing equations for this problem can be formulated as:

$$\frac{\partial u}{\partial x} + \frac{\partial v}{\partial y} = 0 \tag{1}$$

$$u\frac{\partial u}{\partial x} + v\frac{\partial u}{\partial y} = \nu\frac{\partial^2 u}{\partial y^2} - \frac{\sigma B_0^2}{\rho}u + g\beta_T(T - T_\infty) + g\beta_C(C - C_\infty) \tag{2}$$

$$u\frac{\partial T}{\partial x} + v\frac{\partial T}{\partial y} = \alpha\frac{\partial^2 T}{\partial y^2} \tag{3}$$

$$u\frac{\partial C}{\partial x}+v\frac{\partial C}{\partial y} = D\frac{\partial^2 C}{\partial y^2} \tag{4}$$

The boundary conditions for the problem may be written as

$$u(x,0)=U_0, v(x,0)=0, -k\frac{\partial T}{\partial y}(x,0)=h_f(T_f-T(x,0)), C_w(x,0)=Ax^{\lambda}+C_{\infty}$$
$$u(x,\infty)=0,\ T(x,\infty)=T_{\infty},\ C(x,\infty)=C_{\infty} \tag{5}$$

The *Cauchy-Riemann equations* satisfy the continuity equation (1) with:

$$u=\frac{\partial \psi}{\partial y} \text{ and } v=-\frac{\partial \psi}{\partial x} \tag{6}$$

$$\eta=y\sqrt{\frac{U_0}{\nu x}}\ ,\quad \psi=\sqrt{\nu x U_0}f(\eta) \tag{7}$$

Where the plate velocity is denoted by U_0, the symbols ν, C_∞, α,D, β_T, β_C, ρ, g, σ, ψ, η have their appropriate elucidations.

The *temperature* and *concentration* in non-dimensional form are given as

$$\theta(\rho)=\frac{T-T_{\infty}}{T_f-T_{\infty}},\quad \phi(\rho)=\frac{C-C_{\infty}}{C_f-C_{\infty}} \tag{8}$$

The non-dimensional ordinary governing differential equations are:

$$f'''+\frac{1}{2}ff''-Mf'+Gr\theta+Gm\phi = 0 \tag{9}$$

$$\theta''+\frac{1}{2}Prf\theta' = 0 \tag{10}$$

$$\phi''+\frac{1}{2}Scf\phi' = 0 \tag{11}$$

Applicable boundary conditions are

$$f(0)=0, f'(0)=1, \theta'(0)=Bi[\theta(0)-1], \phi(0)=1 f(\infty)=0, \theta(\infty)=\phi(\infty)=0 \tag{12}$$

3. Method of Solution

According to the HPM, the Homotopy form of equations from (9)-(11) can be written as

$$(1-p)(f'''-Mf'+Gr\theta+Gm\phi)+$$
$$p\left(f'''+\frac{1}{2}ff''-Mf'+Gr\theta+Gm\phi\right) = 0 \tag{13}$$

$$(1-p)(\theta^{''}) + p\left(\theta^{''} + \frac{1}{2}Prf\theta'\right) = 0 \quad (14)$$

$$(1-p)(\phi^{''}) + p\left(\phi^{''} + \frac{1}{2}Scf\phi'\right) = 0 \quad (15)$$

Let us consider $f,\ \theta,\ \phi$ as

$$f = f_0 + pf_1 + p^2 f_2 + ... \quad (16)$$
$$\theta = \theta_0 + p\theta_1 + p^2\theta_2 + ... \quad (17)$$
$$\phi = \phi_0 + p\phi_1 + p^2\phi_2 + ... \quad (18)$$

Substituting (16)-(18) into the equations (13)-(15) and rearranging the various powers of p , we get

Terms independent of p:

$$f_0^{'''} - Mf_0^{'} + Gr\theta_0 + Gm\phi_0 = 0 \quad (19)$$
$$\theta_0^{''} = 0 \quad (20)$$
$$\phi_0^{''} = 0 \quad (21)$$

The boundary conditions are

$$\begin{aligned} f_0(0) = 1,\ f_0^{'}(0) = 1,\ \theta_0(0) = Bi[\theta_0(0) - 1],\ \phi_0(0) = 1 \\ f_0^{'}(\infty) = 0,\ \theta_0(\infty) = \phi_0(\infty) = 0 \end{aligned} \quad (22)$$

Terms containing p only:

$$f_1^{'''} - Mf_1^{'} + Gr\theta_1 + Gm\phi_1 + \frac{1}{2}f_0 f_0^{''} = 0 \quad (23)$$
$$\theta_1^{''} + \frac{1}{2}Prf_0\theta_0' = 0 \quad (24)$$
$$\phi_1^{''} + \frac{1}{2}Scf_0\phi_0' = 0 \quad (25)$$

The boundary conditions are

$$\begin{aligned} f_1(0) = 0,\ f_1^{'}(0) = 0,\ \theta_1^{'}(0) = Bi[\theta_1(0)],\ \theta_1(0) = 0 \\ f_1^{'}(\infty) = 0,\ \theta_1(\infty) = 0,\ \phi_1(\infty) = 0 \end{aligned} \quad (26)$$

Solving equations (19)-(21) under the boundary conditions (22) and (23)-(25) under the boundary conditions (26), we have

$$\theta_0 = C_1\eta + C_2 \tag{27}$$

$$\phi_0 = C_3\eta + C_4 \tag{28}$$

$$f_0 = C_5 + C_6 e^{-\sqrt{a}\eta} + C_7 e^{\sqrt{a}\eta} + A_3\eta^2 + A_4\eta \tag{29}$$

$$\theta_1 = -\frac{1}{2}dC_1\left(\frac{C_5}{2}\eta^2 + \frac{C_6}{a}e^{-\sqrt{a}\eta} + \frac{C_7}{a}e^{\sqrt{a}\eta} + \frac{A_3}{12}\eta^4 + \frac{A_3}{12}\eta^4 + \frac{A_4}{6}\eta_3\right) + C_8\eta + C_9 \tag{30}$$

$$\phi_1 = -\frac{1}{2}eC_3\left(\frac{C_5}{2}\eta^2 + \frac{C_6}{a}e^{-\sqrt{a}\eta} + \frac{C_7}{a}e^{\sqrt{a}\eta} + \frac{A_3}{12}\eta^4 + \frac{A_3}{12}\eta^4 + \frac{A_4}{6}\eta_3\right) + C_{10}\eta + C_{11} \tag{31}$$

$$f_1 = C_{15} + C_{13}e^{\sqrt{a}\eta} + C_{14}e^{-\sqrt{a}\eta} + A_{20}\eta + A_{21}\eta^2 + A_{22}\eta^3 + A_{23}\eta^4 + A_{25}\eta e^{\sqrt{a}\eta} + A_{26}\eta e^{-\sqrt{a}\eta} + A_{27}\eta^2 e^{\sqrt{a}\eta} + A_{28}\eta^2 e^{-\sqrt{a}\eta} + A_{29}\eta^3 e^{\sqrt{a}\eta} + A_{30}\eta^3 e^{-\sqrt{a}\eta} + A_{31}e^{-2\sqrt{a}\eta} + A_{32}e^{2\sqrt{a}\eta} \tag{32}$$

Neglecting higher order perturbed terms we finally obtain:

$$f = f_0 + pf_1, \quad \theta = \theta_0 + p\theta_1, \quad \phi = \phi_0 + p\phi_1$$

4. Results and Discussion

In this study, the numerical results are obtained for different values of parameters Gr, Gm, Bi_x, Sc, M, Pr with fixed value of *Homotopy Perturbation Parameter* ($p = 0.1$) implanted in the flow system.

Figures 2-5 describe the fluid velocity against η. The effects of various values of magnetic parameter (M), Schimdt number (Sc), Prandtl number (Pr) and heat exchange parameter (Bi_x) on velocity profile are revealed. Figure 2 demonstrates that with the enhancement of magnetic field parameter, the fluid velocity moves down monotonically to the free stream value zero far away from the plate satisfying the boundary condition. This happens because the presence of magnetic field in an electrically conducting fluid generates a force called the Lorentz force which acts against the flow if the magnetic field is applied in the normal direction. This result clearly interprets the physical behaviour of the magnetic field parameter. Figure 3 depicts that the velocity transport of the fluid medium is enriched for low mass diffusivity of the species. From figure 4, it is observed that Prandtl number controls the fluid flow indicating the fact that thermal diffusivity leads to a crumbling thermal boundary layer thickness. The retardation behaviour of fluid velocity under the action of heat exchange parameter is described in figure 5.

Figures 6-9 depict the temperature profile against η. It is seen from figure 6 that the temperature profile rises due to the acceleration of magnetic intensity. This happens because the variation of magnetic field induces a localized electric current which generates heat in the fluid medium. An enhancement of convective heat exchange parameter (Bi_x), produces greater temperature near the plate and the falling down behaviour of the temperature field far away from the plate is observed in figure 7. It is obvious because as the fluid is heated up near the plate, the plate becomes lighter and the flow faster. In the same way, the flow moves slower as we move far away from the plate as the effect of the heated plate is negligible. Figure 8 exhibits that with the higher values of thermal diffusivity, the fluid temperature is reduced satisfying the boundary condition. It is mainly because of the distortion of the network. i.e higher the temperature the more hindered the fluid particles are. This causes the thermal conductivity of the flow pattern to minimize itself. From figure 9, it is found that thermal buoyancy force reduces the fluid temperature. It is obvious as higher the thermal buoyancy force, grater is the density of the fluid particles, resulting in a reduction of the temperature of flow pattern.

The concentration profile rises due to the strength of the applied magnetic field which is experienced in Figure 10. The effects of the *Schmdit number* (Sc), Thermal *Grashof number* (Gr) and *Solutal Grashof number* (Gm) on species concentration have been incorporated in figures 11-13. It is inferred from these figures that the concentration level of the fluid drops for low *mass diffusivity, thermal* and *solutal buoyancy force.*

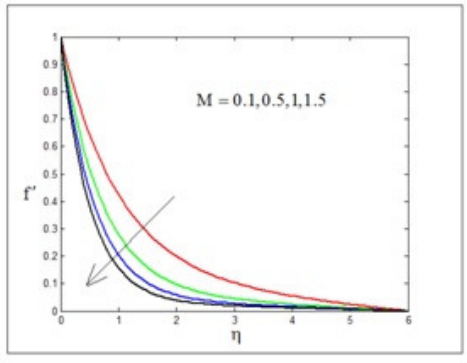

Figure 2: Velocity versus η under $Gr = 0.1,\ Gm = 0.1,\ Bi_x = 0.1,$ $Sc = 0.62,\ Pr = 0.72,\ P = 0.1$

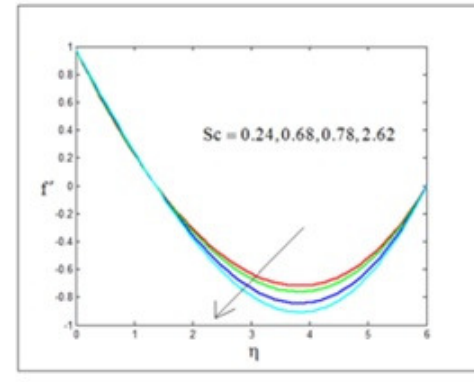

Figure 3: Velocity versus η under $Gr = 0.1,\ Gm = 0.1,\ Bi_x = 0.1,\ M = 0.1,\ Pr = 0.72,\ P = 0.1$

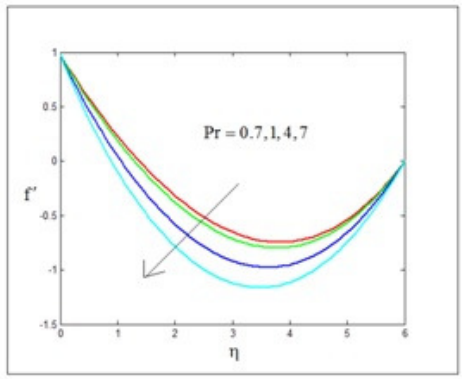

Figure 4: Velocity versus η under $Gr = 0.1,\ Gm = 0.1,\ Bi_x = 0.1,$ $Sc = 0.62,\ M = 0.1,\ P = 0.1$

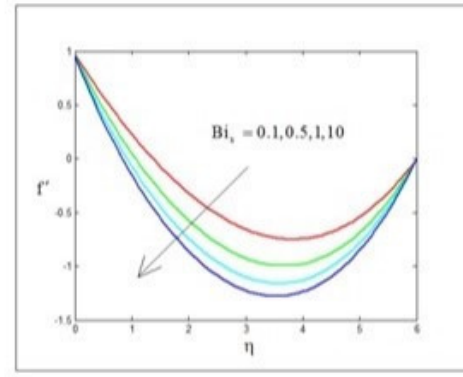

Figure 5: Velocity versus η under $Gr = 0.1,\ Gm = 0.1,\ Pr = 0.72,\ Sc = 0.62,\ M = 0.1,\ P = 0.1$

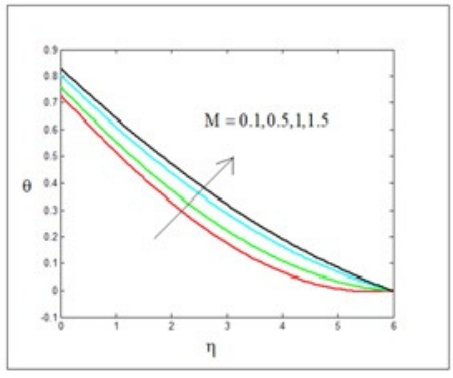

Figure 6: Temperature versus η under $Gr = 0.1,\ Gm = 0.1,\ Bi_x = 0.1,$ $Sc = 0.62,\ Pr = 0.72,\ P = 0.1$

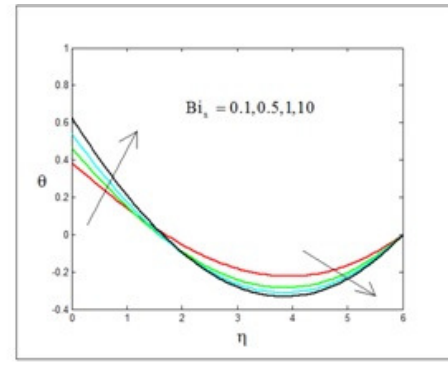

Figure 7: Temperature versus η under $Gr = 0.1,\ Gm = 0.1,\ M = 0.1,\ Sc = 0.62,\ Pr = 0.72,\ P = 0.1$

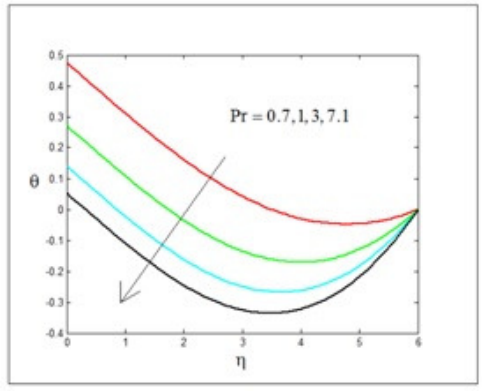

Figure 8: Temperature versus η under $Gr = 0.1,\ Gm = 0.1,\ Bi_x = 0.1,$ $Sc = 0.62,\ M = 0.1,\ P = 0.1$

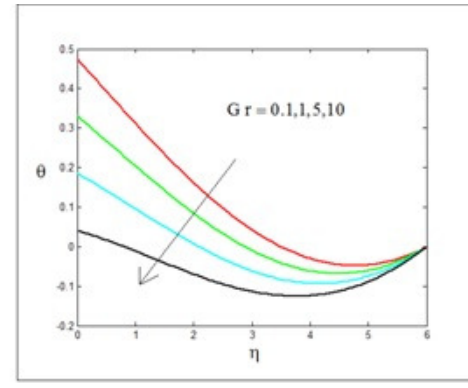

Figure 9: Temperature versus η under $M = 0.1,\ Gm = 0.1,\ Bi_x = 0.1,\ Sc = 0.62,\ Pr = 0.72,\ P = 0.1$

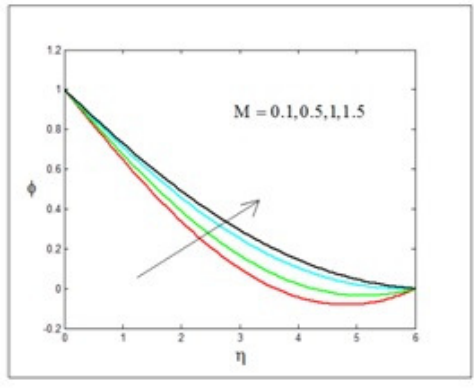

Figure 10: Concentration versus η under $Gr = 0.1,\ Gm = 0.1,\ Bi_x = 0.1,$ $Sc = 0.62,\ Pr = 0.72M = 0.1,\ P = 0.1$

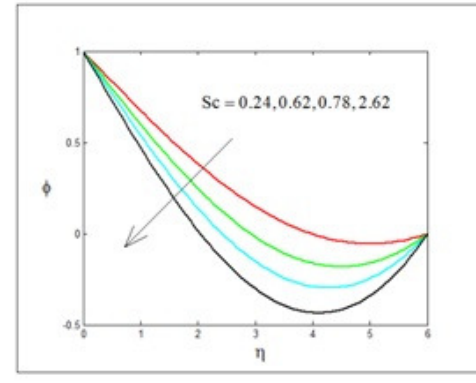

Figure 11: Concentration versus η under $Gr = 0.1,\ Gm = 0.1,\ Bi_x = 0.1,\ M = 0.1,\ Pr = 0.72,\ P = 0.1$

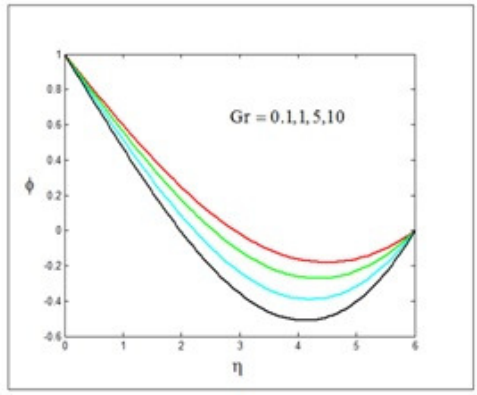

Figure 12: Concentration versus η under $M = 0.1,\ Gm = 0.1,\ Bi_x = 0.1,$ $Sc = 0.62,\ Pr = 0.72,\ P = 0.1$

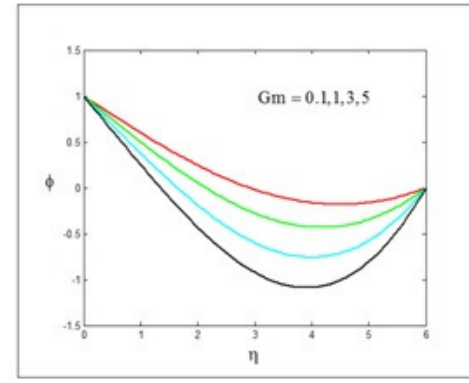

Figure 13: Concentration versus η under $Gr = 0.1,\ M = 0.1,\ Bi_x = 0.1,\ Sc = 0.62,\ Pr = 0.72,\ P = 0.1$

Comparison of graphs with O. D. Makinde [7]:

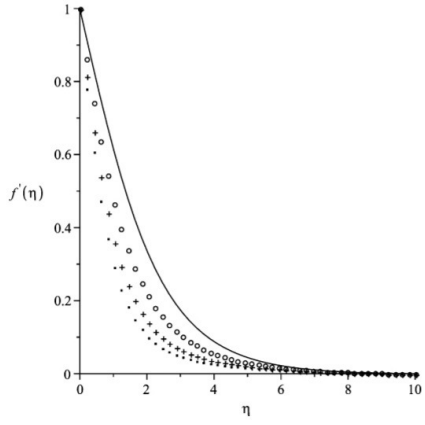

Figure 14: [**Figure 2 in [7]**] Velocity profile for $Pr = 0.72,\ Sc = 0.62,\ Gr_x = Gc_x = Bi_x = 0.1;\ -Ha_x = 0.1; \circ\circ\circ\circ\ Ha_x = 0.5;$ $+++ Ha_x = 1.0; \cdots\cdots\ Ha_x = 1.5$

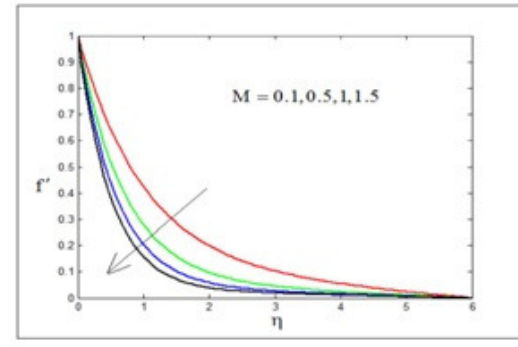

Figure 15: Velocity versus η under $Gr = 0.1,\ Gm = 0.1,\ Bi_x = 0.1,\ Sc = 0.62,$ $Pr = 0.72,\ P = 0.1$

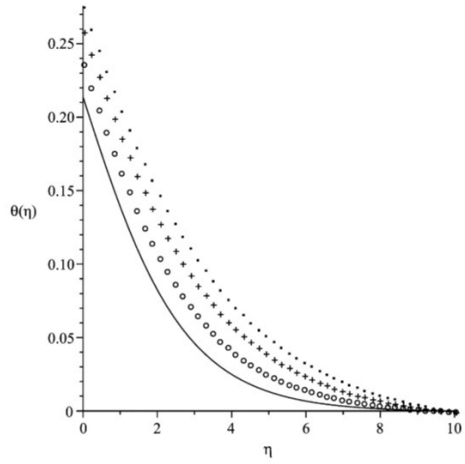

Figure 16: [**Figure 7 in [7]**]
Temperature profiles for
$Pr = 0.72,\ Sc = 0.62,\ Gr_x = Gc_x = Bi_x = 0.1;\ -Ha_x = 0.1; \circ\circ\circ\circ\ Ha_x = 0.5;\ +++\ Ha_x = 1.0; \cdots\cdots\ Ha_x = 1.5$

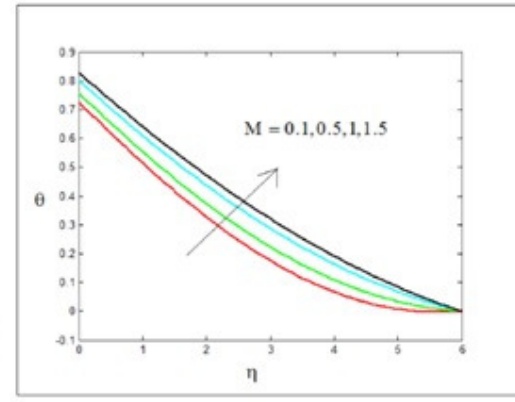

Figure 17: Temperature versus η under $Gr = 0.1,\ Gm = 0.1,\ Bi_x = 0.1,\ Sc = 0.62,$
$Pr = 0.72,\ P = 0.1$

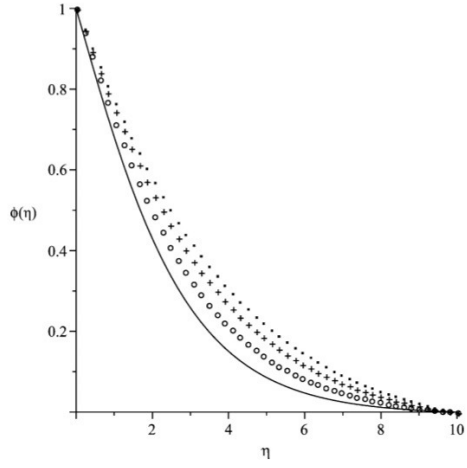

Figure 18: [**Figure 13 in [7]**]
Concentration profiles for
$Pr = 0.72,\ Sc = 0.62,\ Gr_x = Gc_x = Bi_x = 0.1;\ -Ha_x = 0.1; \circ\circ\circ\circ\ Ha_x = 0.5;\ +++\ Ha_x = 1.0; \cdots\cdots\ Ha_x = 1.5$

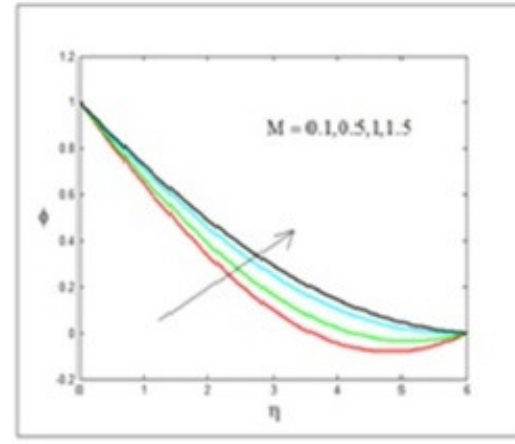

Figure 19: Concentration versus η under $Gr = 0.1,\ Gm = 0.1,\ Bi_x = 0.1,\ Sc = 0.62,$
$Pr = 0.72,\ P = 0.1$

5. Comparison of Results

The work of O. D. Makinde [7] is considered for comparing the results of the present paper.

Comparing figures 15, 17 and 19 with the figures 2 (here, figure 14), 7 (here, figure 16) and 13 (here, figure 18) of the work done by O. D. Makinde [7], we observe the same kind of behaviour due to the implementation of Magnetic intensity in velocity, temperature and concentration profiles for fixed values of $Gr = 0.1$, $Gm = 0.1$, $Bi_x = 0.1$, $Sc = 0.62$, $Pr = 0.72$,$P = 0.1$ i.e. there is a significant effect of Hartmann number on these profiles. Thus, there is an excellent agreement between the results obtained by O. D. Makinde [7] and those arrived at by the present authors.

6. Concluding Remarks

In this paper, the problem of MHD boundary layer flow over a moving vertical plate in presence of heat and mass transfer is considered by HPM. The obtained results are revealed graphically and are compared with the accurate solutions. The result shows that the estimated solution obtained in this paper has excellent agreement with the work done in [7].

References

[1] Aziz, A., A Similarity for laminar thermal boundary layer over a flat plate with convective surface boundary condition, Commun. Nonlinear Sci. Numer. Simulat, 14 (2009), 1064-1068.

[2] Chamkha, A. J. and Khaled, A. A., Similarity solutions for hydromagnetic mixed convection heat and mass transfer for hiemenz flow through porous media, Int. J. Numer. Meth. Heat Fluid Flow, 10(1) (2000), 94-115.

[3] Cortell, R., MHD flow and mass transfer of an electrically conducting fluid of second grade in a porous medium over a stretching sheet with chemically reactive species for two classes of visco-elastic fluid over a porous stretching sheet, Chem. Eng. Process, 46 (2007), 721-728.

[4] He, J.H., An elementary introduction to the homotopy perturbation method, Comp. Math. Appl., 57(3) (2009), 410-412.

[5] Jhankal, A. K., Homotopy perturbation method for MHD boundary layer flow with low pressure gradient over a flat plate, J. Appl. Fluid Mech., 7 (2014), 177-185.

[6] Magyari, E., A moving plate thermometer, Int. J. Therm. Sci., 47 (2008), 1436-1441.

[7] Makinde, O. D., On MHD heat and mass transfer over a moving vertical plate with a convective surface boundary condition, Can. J. Chem. Eng., 88 (2010), 983-990.

[8] Postelnicu, A., Influence of a magnetic field on heat and mass transfer by natural convection from vertical surface in porous media considering soret and doufour effects, Int. J. Heat Mass Transfer., 47 (2004),1467-1472.

[9] Sinha. S, Sarma. M. K, Effect of streatching parameter in a non-linear MHD Flow close to stagnation point, J. Math. Comput. Sci, 10, (6) (2020), 2249-2260, https://doi.org/10.28919/jmcs/4859.

[10] Tesfaye, K., Eshetu, H. Gurju A. and Tadesse, W., Heat and mass transfer in unsteady boundary layer flow of Williamson nanofluids, Hindwai Journal of Applied Mathematics, (2020), Article ID 1890972, 13 pages, https// doi.org/ 10.1155/ 2020/ 1890972.

[11] Tesfaye, K., Eshetu, H. Gurju A. and Tadesse, W., Heat and mass transfer analysis in unsteady flow of tangent hyperbolic nanofluid over a moving wedge with buoyancy and dissipation effects, Heliyon (Elsevier), 6 (2020), https://doi.org/10.1016/j.heliyon.2020.e03776.

[12] White, F., Viscous fluid flow, 3rd ed., McGraw-Hill, New York, (2006).

Appendix

$a = Ha_x,\ b = Gr_x,\ c = Gc_x,\ d = P,\ e = Sc,$

$$C_1 = -\frac{6Bi_x}{1+6Bi_x},\ C_2 = \frac{6Bi_x}{1+6Bi_x},\ C_3 = -\frac{1}{6},\ C_4 = 1,\ C_5 = -\frac{2A_2 - A_1(e^{6\sqrt{a}} + e^{-6\sqrt{a}})}{\sqrt{a}(e^{6\sqrt{a}} - e^{-6\sqrt{a}})}$$

$$C_6 = \frac{A_2 - A_1 e^{6\sqrt{a}}}{\sqrt{a}(e^{6\sqrt{a}} - e^{-6\sqrt{a}})},\ C_7 = \frac{A_2 - A_1 e^{-6\sqrt{a}}}{\sqrt{a}(e^{6\sqrt{a}} - e^{-6\sqrt{a}})},\ C_8 = Bi_x C_9 + A_5,$$

$$C_9 = \frac{dC_1}{6Bi_x + 1}\left[9C_5 + \frac{C_6}{2a}e^{-6\sqrt{a}} + \frac{C_7}{2a}e^{6\sqrt{a}} + 54A_3 + 18A_4\right] - \frac{6}{1+6Bi_x}A_5,$$

$$C_{10} = \frac{eC_3}{12}\left[18C_5 + \frac{C_6}{a}e^{-6\sqrt{a}} + \frac{C_7}{a}e^{6\sqrt{a}} + 108A_3 + 36A_4\right] - C_{11},$$

$$C_{11} = \frac{eC_3}{2}\left(\frac{C_6 + C_7}{a}\right),\ C_{12} = C_{15} - A_{19},\ C_{13} = \frac{B_2 e^{-6\sqrt{a}} - B_3}{e^{6\sqrt{a}} - e^{-6\sqrt{a}}},$$

$$C_{14} = \frac{B_2 e^{6\sqrt{a}} - B_3}{e^{6\sqrt{a}} - e^{-6\sqrt{a}}},\ C_{15} = -2\frac{B_2 e^{-6\sqrt{a}} - B_3}{e^{6\sqrt{a}} - e^{-6\sqrt{a}}} - B_1 - B_2,$$

$$A_1 = 1 - \frac{1}{a}(bC_2 + cC_4),\ A_2 = -\frac{6}{a}(bC_1 + cC_3) - \frac{1}{a}(bC_2 + cC_4),\ A_3 = -\frac{1}{2a}(bC_1 + cC_3),$$

$$A_4 = \frac{1}{a}(bC_2 + cC_4),\ A_5 = -\frac{1}{2}dC_1\left[Bi_x\left(\frac{C_6}{a} + \frac{C_7}{a}\right) + \left(\frac{C_6}{\sqrt{a}} - \frac{C_7}{\sqrt{a}}\right)\right],$$

$$A_6 = bC_9 + cC_{11} + C_5A_3 + aC_6C_7,\ A_7 = \frac{b}{2a}dC_1C_7 + \frac{c}{2a}eC_3C_7 - \frac{a}{2}C_5C_7 - A_3C_7,$$

$$A_8 = \frac{b}{2a}dC_1C_6 + \frac{c}{2a}eC_3C_6 - \frac{a}{2}C_5C_6 - A_3C_6,$$

$$A_9 = bC_8 + cC_{10} + A_3A_4,\ A_{10} = -A_3^2 + \frac{b}{4}dC_1C_5 + \frac{c}{4}eC_3C_4,$$

$$A_{11} = \frac{b}{12}dC_1A_4 + \frac{c}{12}eC_3A_4,\ A_{12} = \frac{b}{24}dC_1A_3 + \frac{c}{24}eC_3A_3,\ A_{13} = \frac{1}{2}aC_6^2,$$

$$A_{14} = \frac{1}{2}aC_7^2,\ A_{15} = \frac{1}{2}aC_7A_4,\ A_{16} = \frac{1}{2}aC_6A_4,\ A_{17} = \frac{1}{2}aC_7A_3,\ A_{18} = \frac{1}{2}aC_6A_3,$$

$$A_{19} = -\frac{1}{a}\left(\frac{6A_{11}}{a^2} - \frac{A_9}{a}\right),\ A_{20} = -\frac{1}{a}\left(\frac{24A_{12}}{a^2} + \frac{2A_{10}}{a} - A_6\right),\ A_{21} = -\frac{1}{a}\left(\frac{3A_{11}}{a} - \frac{A_9}{2}\right),$$

$$A_{22} = -\frac{1}{a}\left(\frac{4A_{12}}{a} + \frac{A_{10}}{3}\right),\ A_{23} = -\frac{1}{a}\frac{A_{11}}{4},\ A_{24} = -\frac{1}{a}\frac{A_{12}}{5},$$

$$A_{25} = \frac{A_7}{2a} + \frac{3A_{15}}{4a\sqrt{a}} - \frac{7A_{11}}{2a^2},\ A_{26} = \frac{A_8}{2a} + \frac{3A_{16}}{4a\sqrt{a}} - \frac{7A_{18}}{2a^2},\ A_{27} = \frac{A_{15}}{4a} - \frac{3A_{18}}{4a\sqrt{a}},$$

$$B_1 = A_{31} + A_{32},\ B_2 = \frac{1}{\sqrt{a}}(A_{20} + A_{25} + A_{26} - 2\sqrt{a}A_{31} + 2\sqrt{a}A_{32})$$

$$\begin{aligned} B_3 = \frac{1}{\sqrt{a}}[&A_{20} + 12A_{21} + 108A_{22} + 864A_{23} + 6480A_{24} \\ &+ \{A_{25}(1 + 6\sqrt{a}) + A_{27}(12 + 36\sqrt{a}) + A_{29}(108 + 216\sqrt{a})\}e^{6\sqrt{a}} \\ &+ \{A_{26}(1 - 6\sqrt{a}) + A_{28}(12 - 36\sqrt{a}) + A_{30}(108 - 216\sqrt{a})\}e^{-6\sqrt{a}} \\ &- A_{31}2\sqrt{a}e^{-12\sqrt{a}} + A_{32}2\sqrt{a}e^{12\sqrt{a}}] \end{aligned}$$